British Journal of Psychiatry (doi: 10.1192/bjp.bp.114.155499)

Online supplement

Methods

Neuropsychological and Clinical Assessment

Hearing was tested with the calibrated finger rub auditory screening test (CALFRAST).[1] All participants completed the Wechsler Test of Adult Reading (WTAR).[2] SP completed the Measurement and Treatment Research to Improve Cognition in Schizophrenia (MATRICS) battery,[3,4] Positive and Negative Syndrome Scale (PANSS),[5] Calgary Depression Scale,[6] Clinical Global Impression (CGI),[7] Fagerstrom Test for Nicotine Dependence (FTND),[8] **Abnormal Involuntary Movements Scale (AIMS)[9] for tardive dyskinesia, a modified version of the Simpson-Angus Scale (SAS) [10] for parkinsonism, Barnes Akathisia Scale (BAS)**,[11] and the UCSD Performance Based Skills Assessment (UPSA-2).[12]

MR Imaging

All images were collected on a Siemens 3 Tesla Tim Trio. High resolution T1-weighted images were acquired with a 5-echo multi-echo MPRAGE sequence [TE (echo times) = 1.64, 3.5, 5.36, 7.22, 9.08 ms, TR (repetition time) = 2.53 s, TI (inversion time) = 1.2 s, 7° flip angle, number of excitations (NEX) = 1, slice thickness = 1 mm, FOV (field of view) = 256 mm, resolution = 256 x 256]. Echo-planar images (EPI) were collected using a single-shot, gradient-echo echoplanar pulse sequence [TR = 2000 ms; TE = 29 ms; flip angle = 75°**;** FOV = 240 mm; matrix size = 64 x 64].

The first three images of each run were eliminated to account for T1 equilibrium effects, resulting in a total of 966 images for the final analyses. Thirty-three contiguous sagittal 3.5-mm thick slices with a gap factor of 1.05 mm were selected to provide whole-brain coverage (voxel size: 3.75 x 3.75 x 4.55 mm).

Analyses

Functional images were generated using Analysis of Functional NeuroImages (AFNI) software package[13] using standard pre-processing steps. Time series images were spatially registered in two- and three-dimensional space to the fourth EPI image of the first run to reduce the effects of head motion, and were temporally interpolated to the first slice to account for differences in slice acquisition. Mean frame-wise displacement was calculated by first converting the 3 rotational motion parameters derived from the rigid body to millimetres using a 50 mm radius sphere.[14] For each image, the absolute difference of the rotational and displacement motion parameters from the previous image was averaged across all images. Two MANOVAs were conducted to examine group differences in translational and rotational frame-wise displacement. Data were then converted to standard stereotaxic coordinate space[15] and spatially blurred using a 8 mm Gaussian full-width half-maximum filter.

A white matter and ventricular exclusion mask was derived from a spatially normalized atlas (FS_Desai_PM from AFNI) containing probabilistic maps of 40 ROI originally parcellated by FreeSurfer.[16] Voxels that exceeded 80% probability of being in white matter or the ventricles (with the exception of 5th ventricle) were first selected to form a template mask, which was then dilated and eroded by 2 mm to fill small holes and smooth edges.

ARMs Analyses

Individual subject T_1 data were first segmented through the standard FreeSurfer reconstruction pipeline (version 5.1). The output was visually inspected to confirm accuracy of registration, surface reconstruction, and segmentation. Regions of interest (ROI) were defined by standard FreeSurfer labels available in the Destrieux atlas.[17] Primary (Heschl's gyrus) and secondary (planum temporale, Heschl's sulcus, planum polare, and superior temporal gyrus)

auditory cortex were defined on the basis of a previous publication.[17] Visual cortex was defined using standard FreeSurfer labels drawn from multiple previous publications.[18,19] Our primary visual cortex parcellation was defined as the V1 label[18] with areas shared by the V2 label[19] removed. For our secondary visual cortex label, we used the entire area identified by Fischl et al.'s V2.[19]

One sample t-tests were first conducted on the resulting distributions to ensure that each ARM was different from the null distribution, which represents a more robust metric for quantifying ARMs. A series of four 2 x 2 ANOVAs were conducted to examine a priori predictions of decreased ARMs for SP at higher frequencies of stimulation. Two SP were extreme outliers for secondary auditory cortex data and were therefore removed from this particular analysis.

Results

Additional Analyses Examining the Effects of Head Motion on Functional Results

Patients exhibited increased head motion relative to HC, and frame-wise displacement was not used as a nuisance regressor in level-one analyses (on individual subject level) per convention in mixed designs.[20] We therefore conservatively focused our primary findings and discussion section on results that survived analyses with frame-wise displacement as a covariate in the full model. However, the use of covariates must be carefully considered for any analyses in which 1) the covariates are significantly different between the groups or 2) where the difference in the covariate is believed to inherently be part of the grouping variable (i.e., disease process). Classic examples of covariates that meet both of these criteria include increased levels of anxiety in depressive disorders and decreased IQ in schizophrenia.[21] As HC and SP differed in

frame-wise displacement in the current study, we repeated all functional analyses without the use of frame-wise displacement as a covariate.

For attend-visual trials, a comparison of the main effect of group from the analytic models that either included (Figure 2) or excluded (see SF 3) frame-wise displacement yielded additional regions of patient hyperactivation within the left auditory cortex, precentral gyrus (BAs 6) and postcentral gyrus (BA 43). In addition, the left lingual gyrus (BAs 18, 19), right paracentral lobule and precuneus (BAs 5,7,31) were also significant, with follow-up analyses indicating that deactivation for HC and baseline activity for SP. A comparison of the group by frequency interaction indicated a significant cluster in the bilateral cerebellum when frame-wise displacement was included in the model relative to a cluster in the right insula extending into the basal ganglia when this term was not included.

For the attend-auditory ANCOVA, additional regions of SP hyperactivation were observed within left secondary auditory cortex (BA 13), left postcentral gyrus and left inferior parietal lobule when frame-wise displacement was not used as a covariate (see SF 8). Increased deactivation for HC was observed within right precuneus, bilateral paracentral lobule (BAs 7,31). The cluster of activation in the left pyramis and cerebellar tonsil of the cerebellum was no longer significant.

Previous studies[14,22] have proposed that participants with excessive motion should be eliminated from analyses. To further reduce the likelihood that current results were secondary to group differences in head motion, an additional 3 HC and 9 SP with greater than 0.50 mean frame-wise displacement were removed from analyses. MANOVAs comparing head motion parameters were not significant in this reduced cohort ($p > 0.10$). fMRI analyses were also repeated for the reduced cohort, with and without frame-wise displacement as a covariate. Our

primary results (i.e., main effect of group) for the reduced group were similar to results with the full cohort currently reported as primary analyses. Results from the Group x Condition interaction also remained negative in the reduced cohort, suggesting that the use of alternative strategies for reducing motion did not significantly affect current results.

Main Effect of Frequency and Second-Order Interactions

The main effects of frequency were in the expected direction (0.66 Hz > 0.33 Hz) and similar for both the attend-visual and attend-auditory trials (see SF 10-12). Briefly, increased activation was observed bilaterally for higher frequency trials within primary and secondary auditory/visual cortex, pre-supplementary and supplementary motor areas, ventrolateral and dorsolateral prefrontal cortex, posterior parietal cortex, thalamus, basal ganglia and bilateral cerebellum (Lobules IV-VII) across both the attend-visual and attend-auditory conditions. More lateralized motor-related activity was also observed in the left sensori-motor cortex and right cerebellum (lobule IX). In addition, increased deactivation was observed within the posterior cingulate gyrus/precuneus (attend-visual trials), left hippocampus (attend-auditory trials) and paracentral lobule (attend-auditory trials) during the high frequency trials.

During attend-visual trials, the condition by frequency interaction was also significant in the right cerebellum (Lobules VIII and VII) for the attend-visual condition, with simple effects testing indicating higher activation for incongruent trials during high ($t_{1,65}$ = -4.75, $p < 0.05$) but not low ($p > 0.10$) frequency stimulation.

The ANOVA for attend-auditory trials also found a significant condition by frequency interaction within the bilateral temporoparietal junction (BAs 19/39/40), driven primarily by increased activation during low relative to high frequency incongruent trials (right: $t_{1,65}$ = 5.98, $p < 0.05$; left: $t_{1,65}$ = 5.41, $p < 0.05$).

References

1 Torres-Russotto D, Landau WM, Harding GW, Bohne BA, Sun K, Sinatra PM. Calibrated finger rub auditory screening test (CALFRAST). *Neurology* 2009; **72**: 1595-600.

2 Wechsler D. *Wechsler Test of Adult Reading: WTAR*. Psychological Corporation, 2001.

3 Kern RS, Nuechterlein KH, Green MF, Baade LE, Fenton WS, Gold JM, et al. The MATRICS Consensus Cognitive Battery, part 2: co-norming and standardization. *Am J Psychiatry* 2008; **165**: 214-20.

4 Nuechterlein KH, Green MF, Kern RS, Baade LE, Barch DM, Cohen JD, et al. The MATRICS Consensus Cognitive Battery, part 1: test selection, reliability, and validity. *Am J Psychiatry* 2008; **165**: 203-13.

5 Kay SR, Fiszbein A, Opler LA. The Positive and Negative Syndrome Scale (PANSS) for schizophrenia. *Schizophrenia Bull* 1987; **13**: 261-76.

6 Addington D, Addington J, Maticka-Tyndale E. Assessing depression in schizophrenia: the Calgary Depression Scale. *Br J Psychiatry Suppl* 1993; 39-44.

7 Guy W. Clinical global impression scale. *The ECDEU Assessment Manual for Psychopharmacology-Revised* 1976; **Volume DHEW Publ No ADM 76, 338**: 218-22.

8 Heatherton TF, Kozlowski LT, Frecker RC, Fagerstrom KO. The Fagerstrom Test for Nicotine Dependence: a revision of the Fagerstrom Tolerance Questionnaire. *Br J Addict* 1991; **86**: 1119-27.

9 Guy W. ECDEU Assessment Manual for Psychopharmacology ADM-76-338. *Washington, DC: US Dept of Health, Education and Welfare* 1976; 534-7.

10 Simpson GM, Angus JW. A rating scale for extrapyramidal side effects. *Acta Psychiatr Scand Suppl* 1970; **212**: 11-9.

11 Barnes TR. A rating scale for drug-induced akathisia. *Br J Psychiatry* 1989; **154**: 672-6.

12 Patterson TL, Goldman S, McKibbin CL, Hughs T, Jeste DV. UCSD Performance-Based Skills Assessment: development of a new measure of everyday functioning for severely mentally ill adults. *Schizophr Bull* 2001; **27**: 235-45.

13 Cox RW. AFNI: Software for analysis and visualization of functional magnetic resonance neuroimages. *Comput Biomed Res* 1996; **29**: 162-73.

14 Power JD, Barnes KA, Snyder AZ, Schlaggar BL, Petersen SE. Spurious but systematic correlations in functional connectivity MRI networks arise from subject motion. *Neuroimage* 2012; **59**: 2142-54.

15 Talairach J, Tournoux P. *Co-planar Steriotaxic Atlas of the Human Brain*. Thieme, 1988.

16 Fischl B, Dale AM. Measuring the thickness of the human cerebral cortex from magnetic resonance images. *Proc Natl Acad Sci U S A* 2000; **97**: 11050-5.

17 Destrieux C, Fischl B, Dale A, Halgren E. Automatic parcellation of human cortical gyri and sulci using standard anatomical nomenclature. *Neuroimage* 2010; **53**: 1-15.

18 Hinds OP, Rajendran N, Polimeni JR, Augustinack JC, Wiggins G, Wald LL, et al. Accurate prediction of V1 location from cortical folds in a surface coordinate system. *Neuroimage* 2008; **39**: 1585-99.

19 Fischl B, Rajendran N, Busa E, Augustinack J, Hinds O, Yeo BT, et al. Cortical folding patterns and predicting cytoarchitecture. *Cereb Cortex* 2008; **18**: 1973-80.

20 Johnstone T, Ores Walsh KS, Greischar LL, Alexander AL, Fox AS, Davidson RJ, et al. Motion correction and the use of motion covariates in multiple-subject fMRI analysis. *Hum Brain Mapp* 2006; **27**: 779-88.

21 Miller GA, Chapman JP. Misunderstanding analysis of covariance. *J Abnorm Psychol* 2001; **110**: 40-8.

22 Power JD, Mitra A, Laumann TO, Snyder AZ, Schlaggar BL, Petersen SE. Methods to detect, characterize, and remove motion artifact in resting state fMRI. *Neuroimage* 2014; **84**: 320-41.

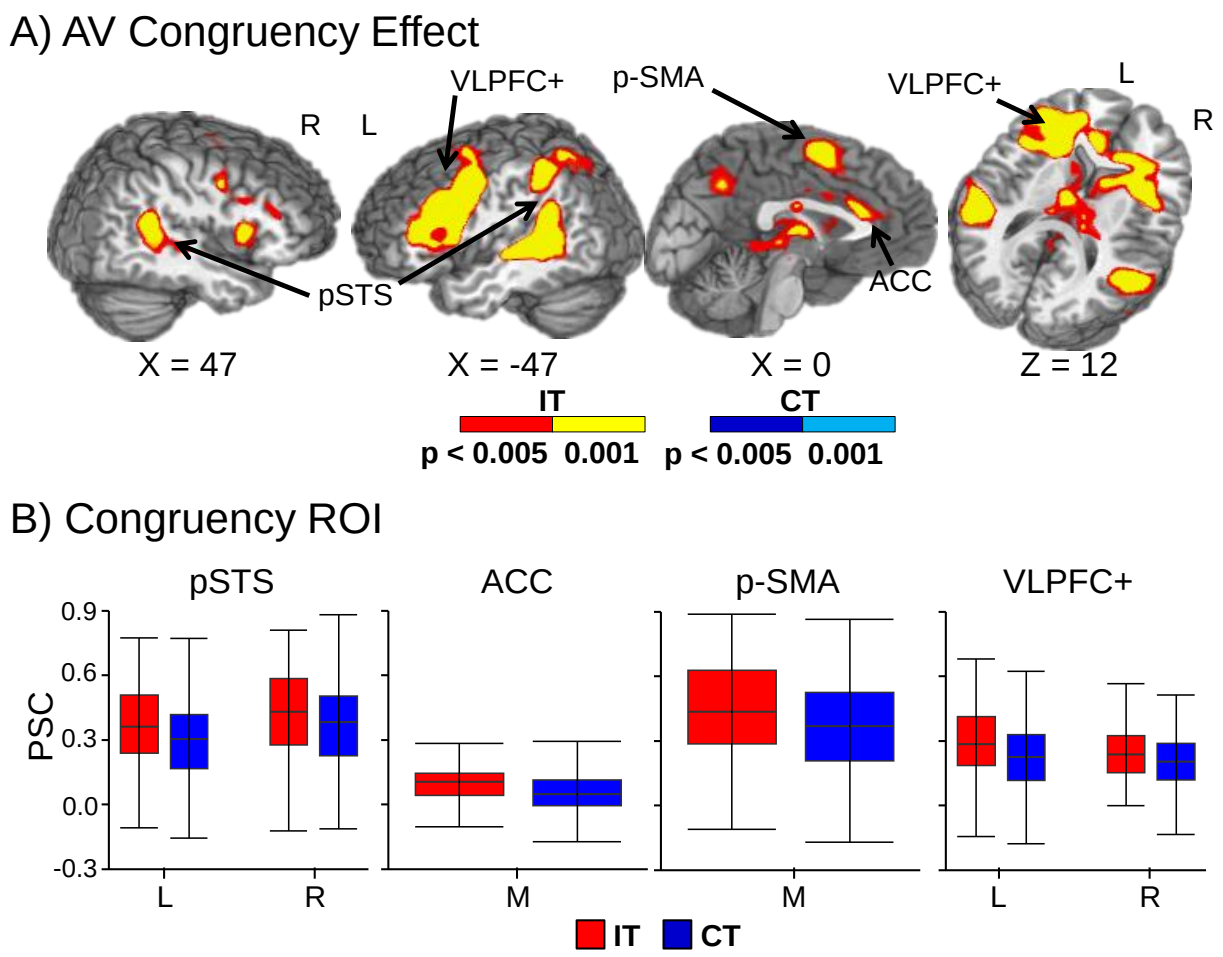

Fig. DS1: This figure presents regions of the brain showing increased activation for incongruent (IT; warm colors) trials relative to congruent (CT; cool colors) trials during the attend-visual (AV) condition (Panel A). Locations of the sagittal (X) and axial (Z) slices are given according to the Talairach atlas for the left (L) and right (R) hemispheres. Panel B presents the box-and-whisker plots for the mean percent signal change (PSC) for selected regions of interest including bilateral posterior superior temporal gyri (pSTS), bilateral anterior cingulate gyrus (ACC), bilateral pre-supplementary motor area (p-SMA) and bilateral ventrolateral and dorsolateral prefrontal cortex (VLPFC+).

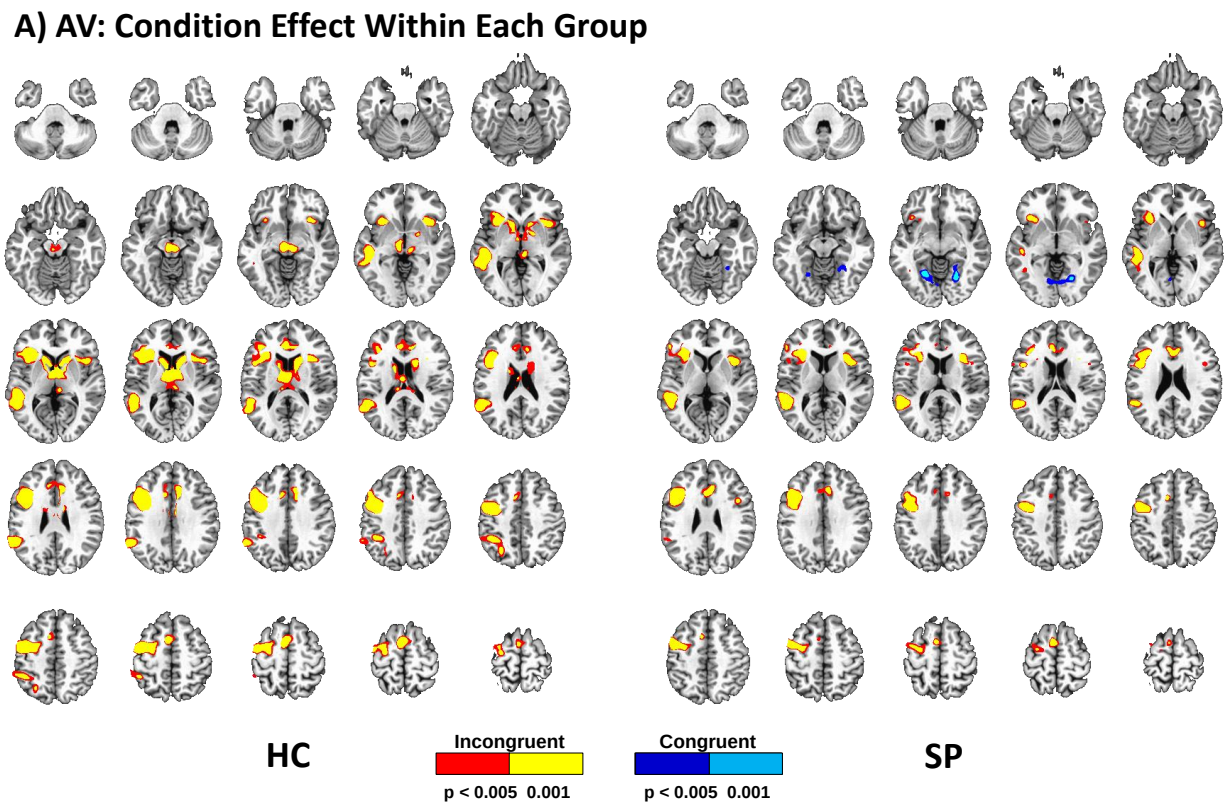

Fig. DS2: This figure presents clusters with significant activation differences between incongruent and congruent trials in the attend-visual (AV) condition. Clusters are presented separately for healthy controls (HC) and patients with schizophrenia (SP) in select axial slices. Clusters are shown in red ($p < 0.005$) and yellow ($p < 0.001$) where activation is greater in incongruent relative to congruent trials and in blue ($p < 0.005$) and cyan ($p < 0.001$) where activation is greater in congruent relative to incongruent trials.

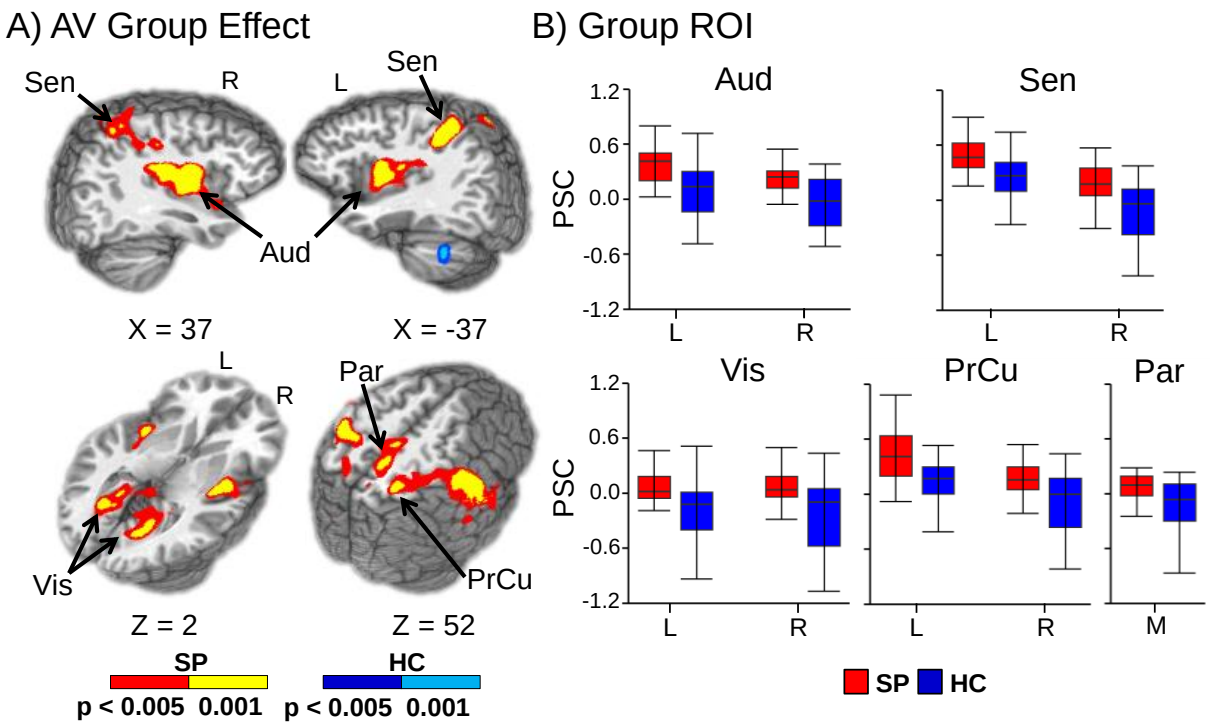

Fig. DS3: Panel A displays the regions of the brain showing significant group differences between patients with schizophrenia (SP = warm colors) and healthy control (HC = cool colors) during the attend-visual (AV) condition when mean frame-wise displacement is excluded as a covariate in analysis. Locations of the sagittal (X) and axial (Z) slices are given according to the Talairach atlas for the left (L) and right (R) hemispheres. Panel B displays box-and-whisker plots of the mean percent signal change (PSC) for selected regions of interest. SP showed increased activation relative to HC within the bilateral auditory cortex (Aud), sensorimotor cortex (Sen) extending into the posterior parietal lobule, and precuneus (PrCu). HC also exhibited deactivation within extrastriate visual cortex (Vis) and paracentral lobule (Par), which was largely absent in SP.

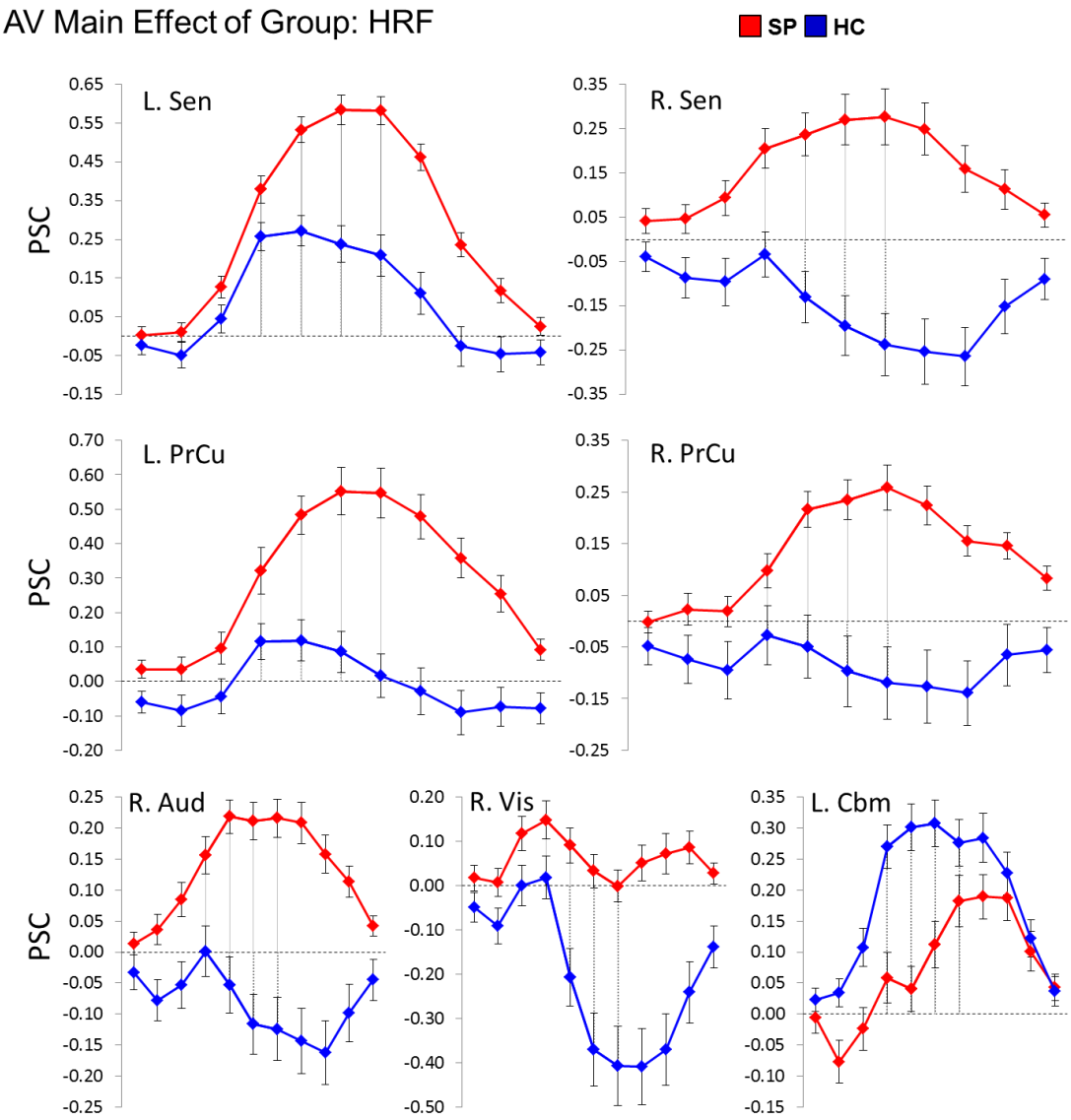

Fig. DS4: This figure presents percent signal change (PSC) data for the entire hemodynamic response function (22-second post-stimulus interval) for patients with schizophrenia (SP = red trace) and healthy controls (HC = blue trace). Panel labels (Sen: sensorimotor cortex; PrCu: precuneus; Aud: auditory cortex; Vis: visual cortex; Cbm: cerebellum) correspond to regions that showed a main effect of group in the attend-visual (AV) condition (see Figure 2). Note that scaling is variable across regions. Error bars are based on the standard error of the mean for each image. The grey drop lines indicate the images that were used to measure the peak hemodynamic response.

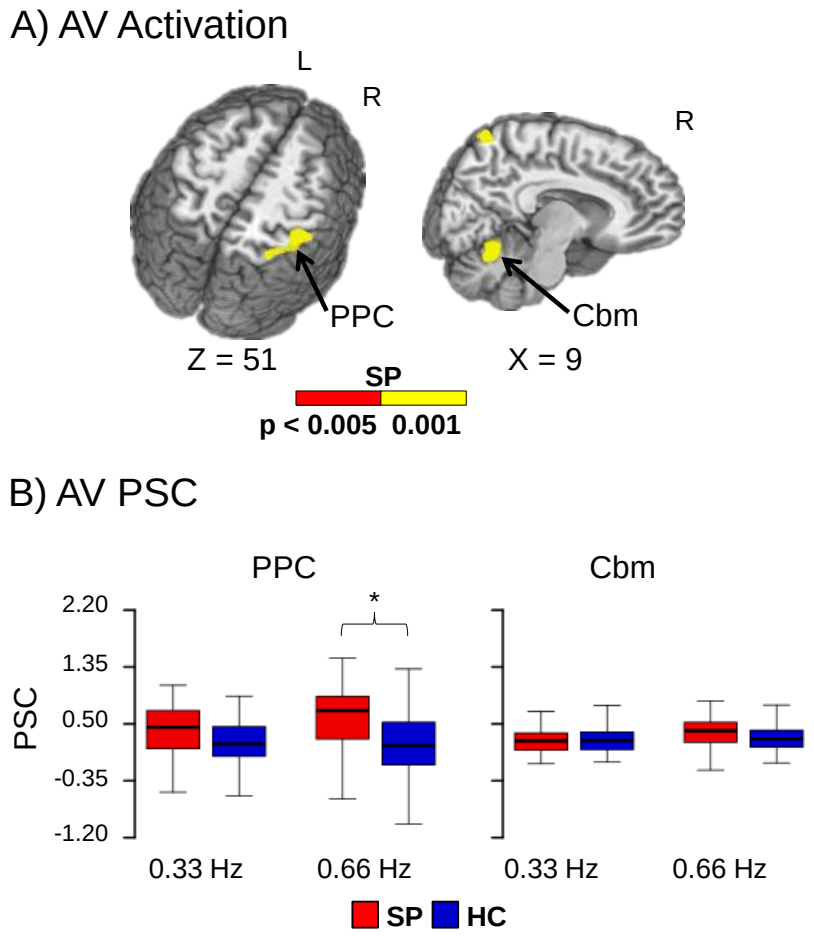

Fig. DS5: Both the right posterior parietal cortex (PPC) and cerebellum (Cbm) exhibited a significant Group x Frequency interaction during the attend-visual (AV) condition (Panel A). The magnitudes of p-values are denoted by red or yellow coloring, and axial slice locations (Z) are given according to the Talairach atlas for both left (L) and right (R) hemispheres. Box-and-whisker plots of the mean percent signal change (PSC) data are presented for both the PPC and Cbm regions for healthy controls (HC = blue) and patients with schizophrenia (SP = red) at 0.33 and 0.66 Hz stimulation frequencies. Asterisk indicates a significant group difference (SP > HC; $p < 0.05$) present at 0.66 Hz stimulus frequency.

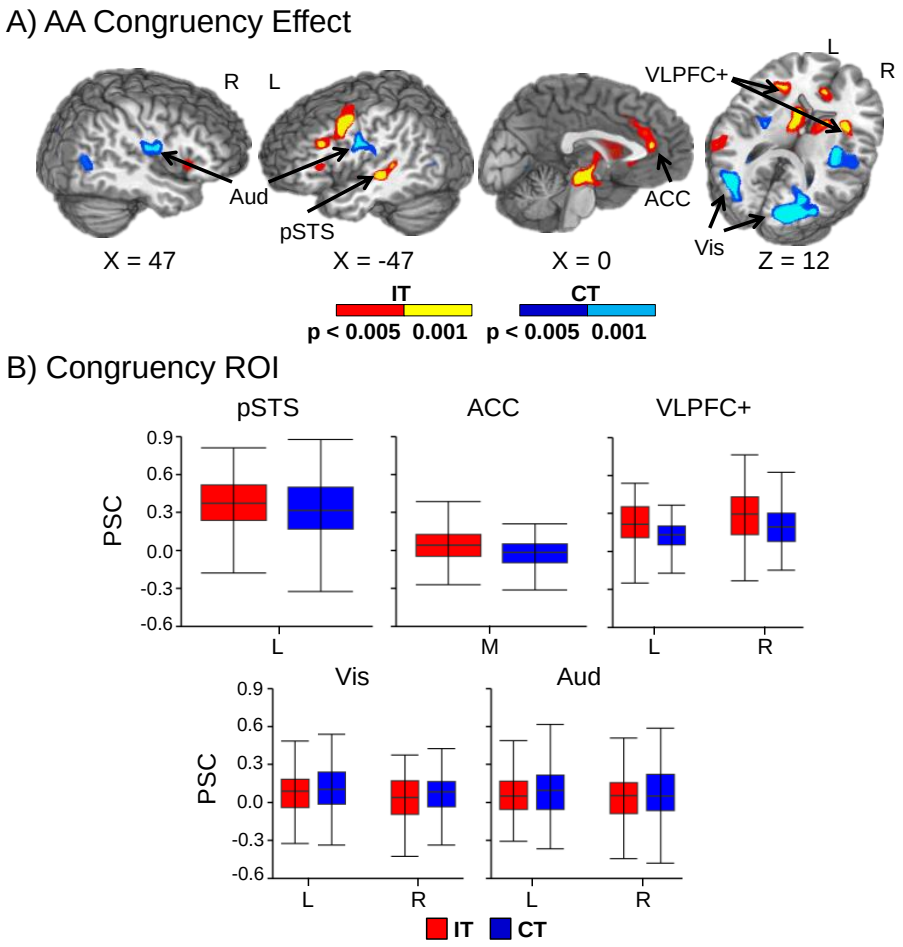

Fig. DS6: During the attend-auditory (AA) condition, there were differential patterns of increased activation for either incongruent (IT; warm colors) or congruent (CT; cool colors) trials (Panel A). Locations of the sagittal (X) and axial (Z) slices are given according to the Talairach atlas for the left (L) and right (R) hemispheres. Panel B presents the box-and-whisker plots for the mean percent signal change (PSC) for selected regions of interest, which generally fell into two different patterns. In the first pattern (top row of Panel B), increased activation was observed within bilateral posterior superior temporal gyri (pSTS), bilateral anterior cingulate gyrus (ACC) and bilateral ventrolateral prefrontal cortex (VLPFC+) for IT relative to CT trials. In the second pattern (Panel B: bottom row), increased activation was observed for CT relative to IT trials within extrastriate visual (Vis) and secondary auditory (Aud) cortex.

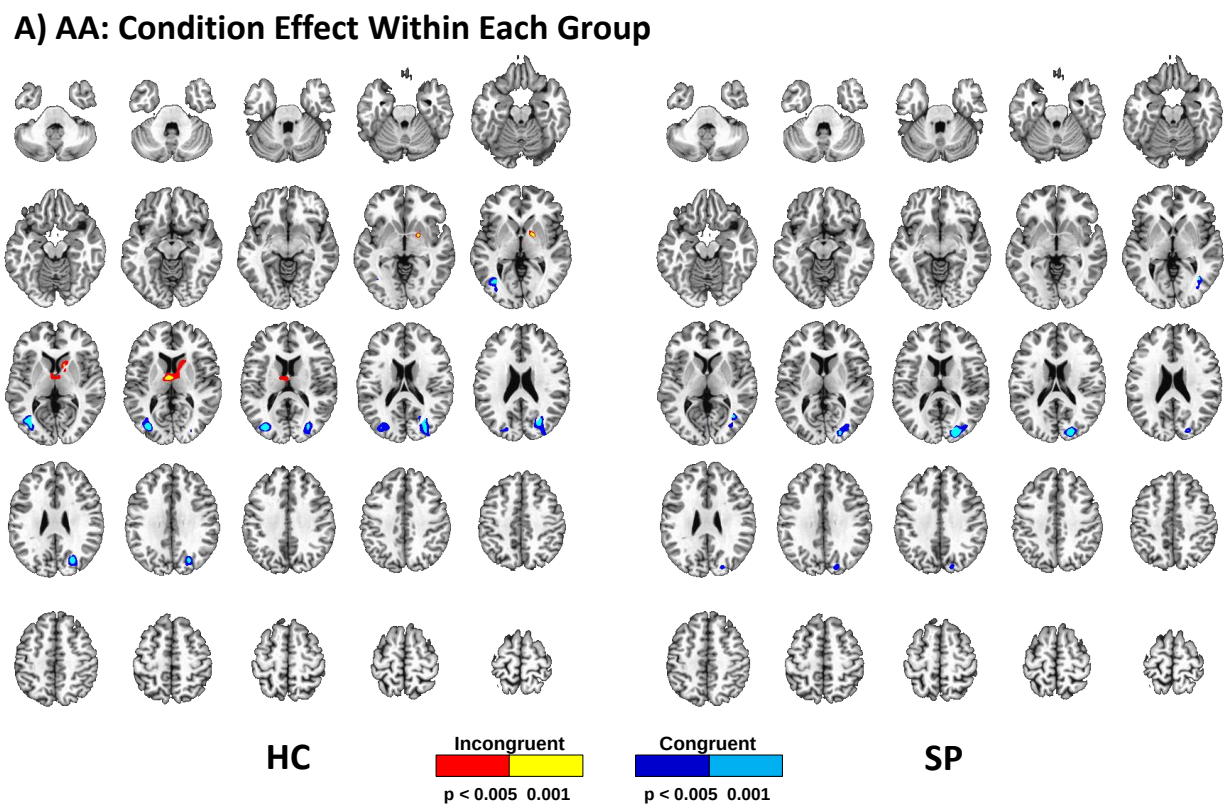

Fig. DS7: This figure presents clusters with significant activation differences between incongruent and congruent trials in the attend-auditory (AA) condition. Clusters are presented separately for healthy controls (HC) and patients with schizophrenia (SP) in select axial slices. Clusters are shown in red ($p < 0.005$) and yellow ($p < 0.001$) where activation is greater for incongruent relative to congruent trials and in blue ($p < 0.005$) and cyan ($p < 0.001$) where activation is greater in congruent relative to incongruent trials.

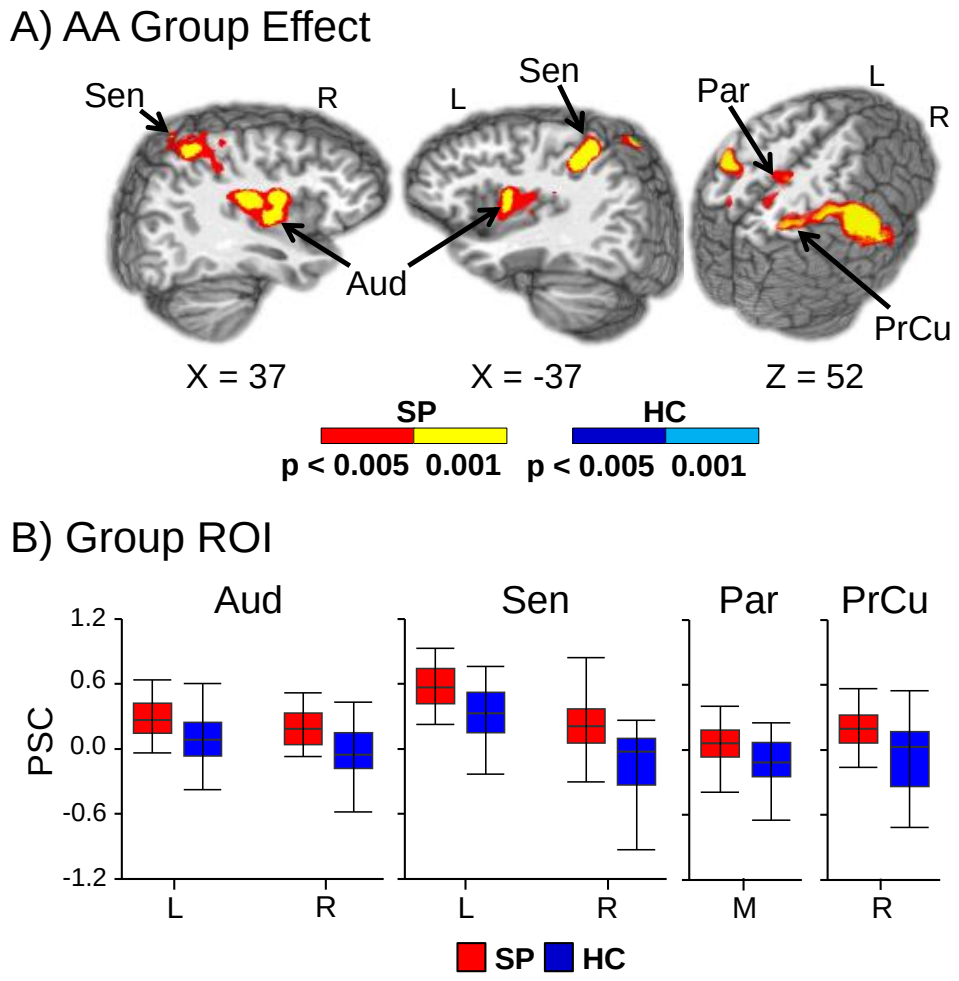

Fig. DS8: Panel A displays the regions of the brain showing significant group differences between patients with schizophrenia (SP = warm colors) and healthy controls (HC = cool colors) during the attend-auditory (AA) condition when mean frame-wise displacement is excluded as a covariate in analysis. Locations of the sagittal (X) and axial (Z) slices are given according to the Talairach atlas for the left (L) and right (R) hemispheres. Panel B presents the box-and-whisker plots for the mean percent signal change (PSC) for selected regions of interest. Increased activation for SP relative to HC was observed within bilateral auditory cortex (Aud), sensorimotor cortex (Sen) extending into the posterior parietal lobule, and right precuneus (PrCu). HC tended to exhibit more deactivation within paracentral lobule (Par) relative to SP.

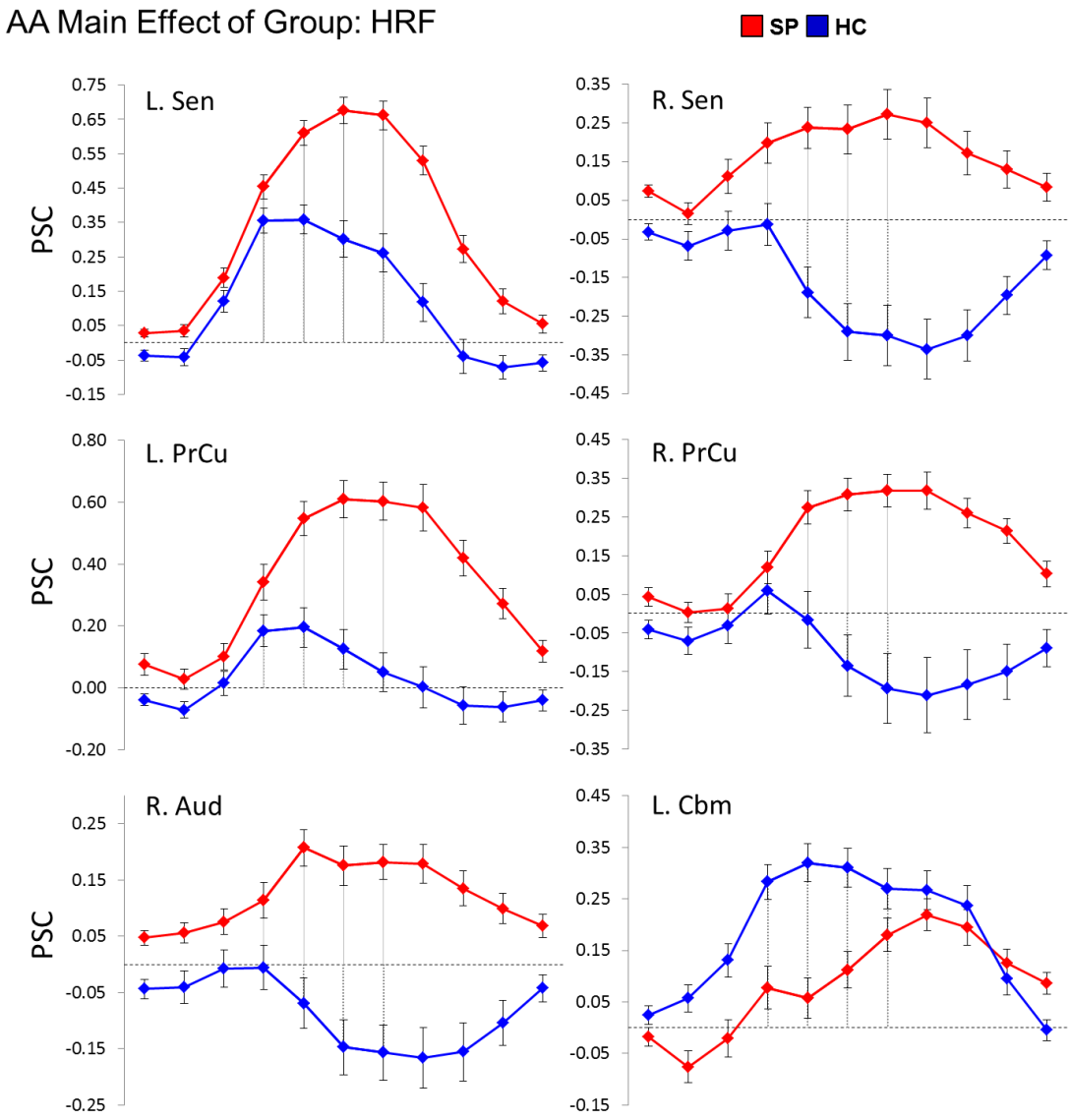

Fig DS9: This figure presents percent signal change (PSC) data for the entire hemodynamic response function (22-second post-stimulus interval) for patients with schizophrenia (SP = red trace) and healthy controls (HC = blue trace). Panel labels (Sen: sensorimotor cortex; PrCu: precuneus; Aud: auditory cortex; Cbm: cerebellum) correspond to regions that showed a main effect of group in the attend-auditory (AA) condition (see Figure 3). Note that scaling is variable across regions. Error bars are based on the standard error of the mean for each image. The grey drop lines indicate the images that were used to measure the peak hemodynamic response.

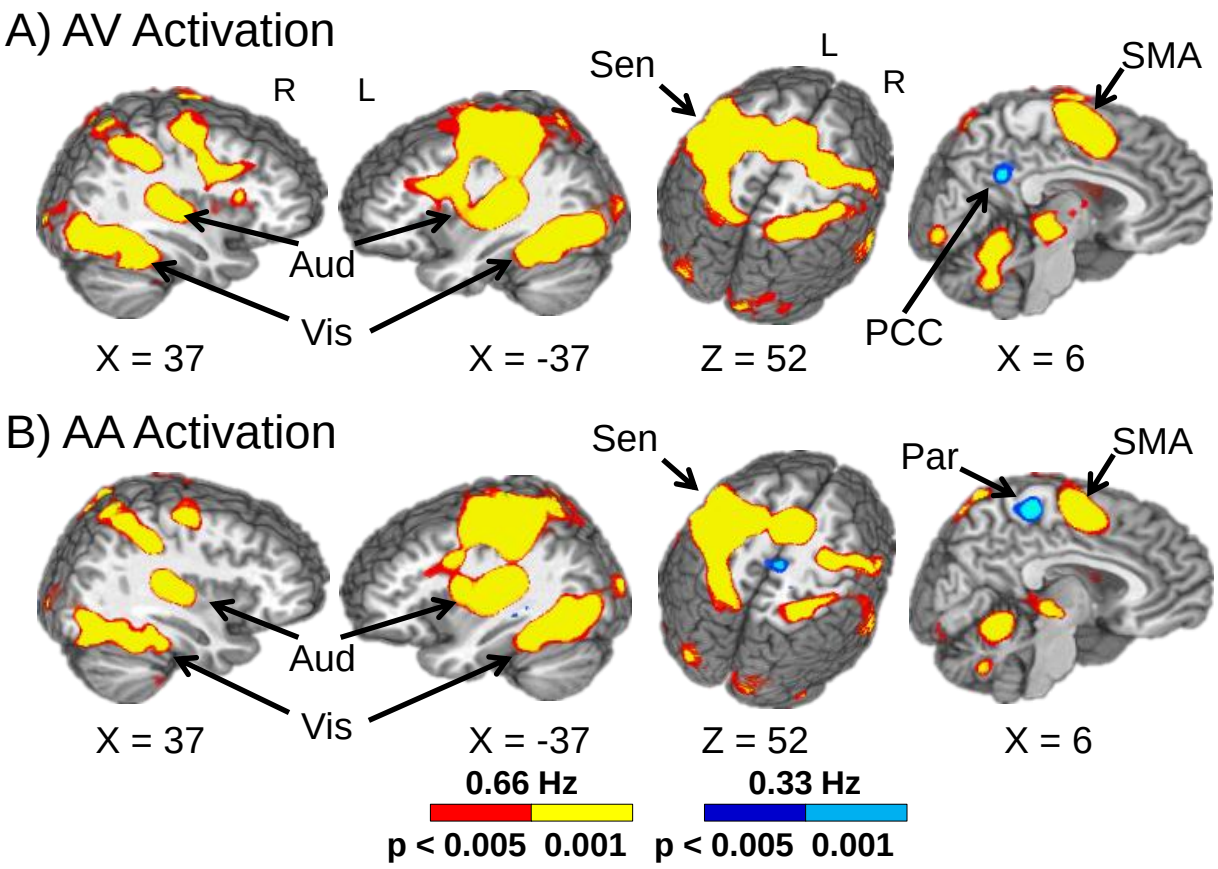

Fig. DS10: This figure displays the brain regions showing significant differences in activation between the low (0.33 Hz: blue/cyan) and high (0.66 Hz = red/yellow) frequency of stimulation trials during the attend-visual (AV; Panel A) and attend-auditory (AA; Panel B) conditions. Locations of the sagittal (X) and axial (Z) slices are given according to the Talairach atlas. Higher frequency trials resulted in increased activation within auditory (Aud), visual (Vis) and sensorimotor (Sen) cortex, as well as supplementary motor areas (SMA), cerebellum and heteromodal cortical areas. Increased deactivation was observed during the high frequency trials within the posterior cingulate gyrus/precuneus (PCC; AV trials), left hippocampus (AA trials) and paracentral lobule (Par; AA trials).

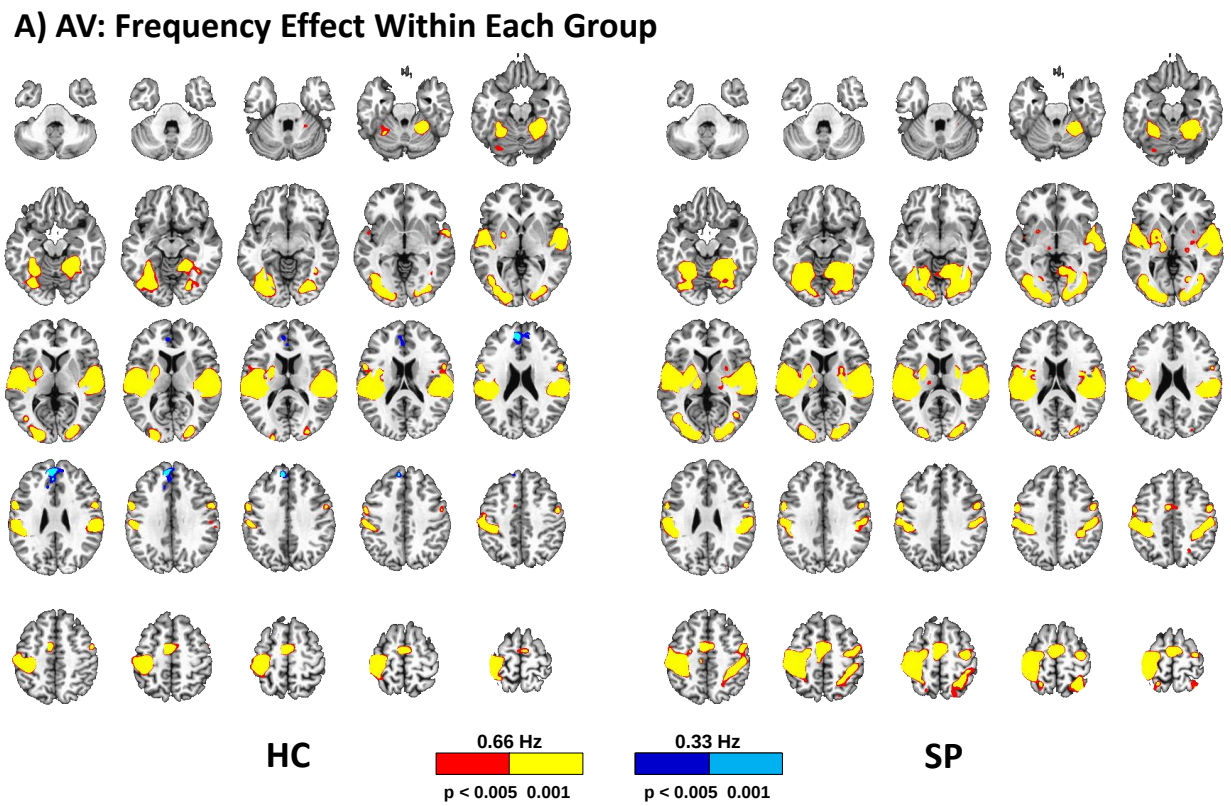

Fig. DS11: This figure presents clusters with significant activation differences between low and high frequency trials in the attend-visual (AV) condition. Clusters are presented separately for healthy controls (HC) and patients with schizophrenia (SP) in select axial slices. Clusters are shown in red ($p < 0.005$) and yellow ($p < 0.001$) where activation is greater in high relative to low frequency trials and in blue ($p < 0.005$) and cyan ($p < 0.001$) where activation is greater in low relative to high frequency trials.

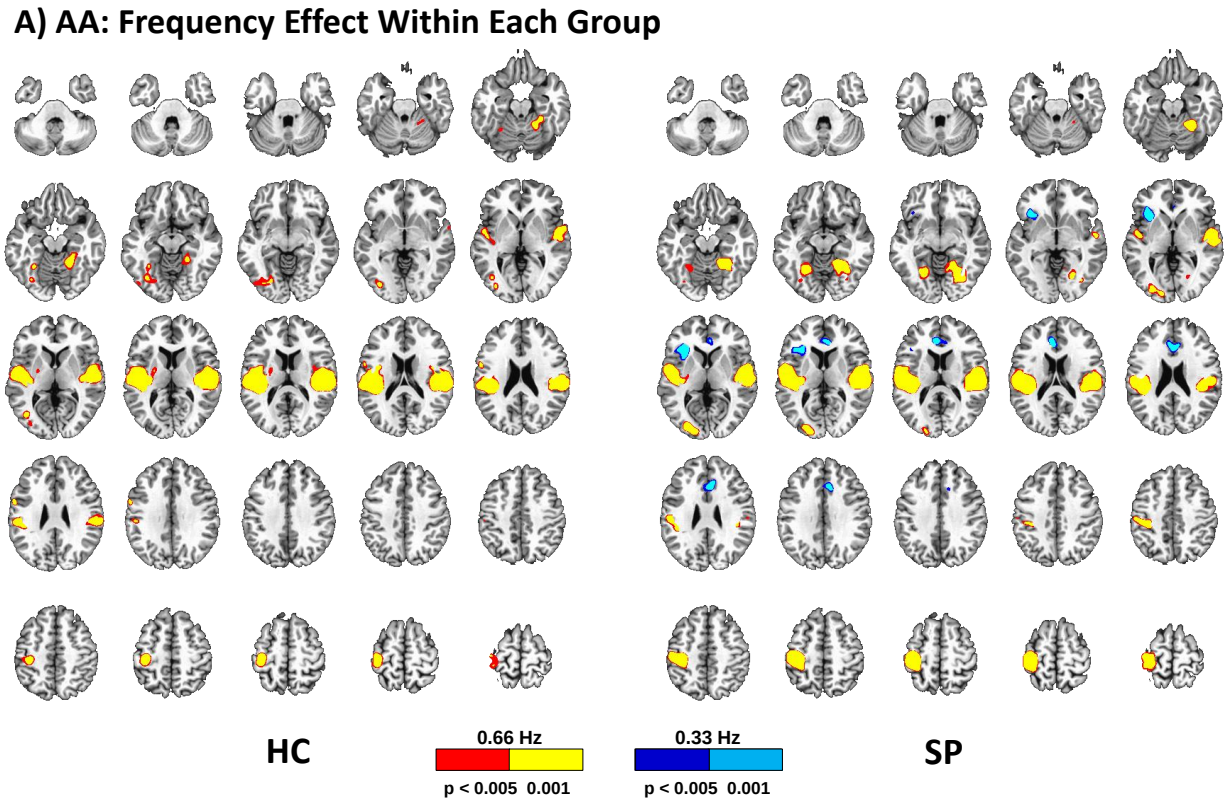

Fig, DS12: This figure presents clusters with significant activation differences between low and high frequency trials in the attend-auditory (AA) condition. Clusters are presented separately for healthy controls (HC) and patients with schizophrenia (SP) in select axial slices. Clusters are shown in red ($p < 0.005$) and yellow ($p < 0.001$) where activation is greater in high relative to low frequency trials and in blue ($p < 0.005$) and cyan ($p < 0.001$) where activation is greater in low relative to high frequency trials.